nature immunology

Lysine methylation of the NF-κB subunit RelA by SETD6 couples activity of the histone methyltransferase GLP at chromatin to tonic repression of NF-κB signaling

Dan Levy[1], Alex J Kuo[1], Yanqi Chang[2], Uwe Schaefer[3], Christopher Kitson[4], Peggie Cheung[1], Alexsandra Espejo[5], Barry M Zee[6], Chih Long Liu[1,7], Stephanie Tangsombatvisit[7], Ruth I Tennen[8], Andrew Y Kuo[1], Song Tanjing[9], Regina Cheung[7], Katrin F Chua[8,10], Paul J Utz[7], Xiaobing Shi[9], Rab K Prinjha[4], Kevin Lee[4], Benjamin A Garcia[6], Mark T Bedford[5], Alexander Tarakhovsky[3], Xiaodong Cheng[2] & Or Gozani[1]

Signaling via the methylation of lysine residues in proteins has been linked to diverse biological and disease processes, yet the catalytic activity and substrate specificity of many human protein lysine methyltransferases (PKMTs) are unknown. We screened over 40 candidate PKMTs and identified SETD6 as a methyltransferase that monomethylated chromatin-associated transcription factor NF-κB subunit RelA at Lys310 (RelAK310me1). SETD6-mediated methylation rendered RelA inert and attenuated RelA-driven transcriptional programs, including inflammatory responses in primary immune cells. RelAK310me1 was recognized by the ankryin repeat of the histone methyltransferase GLP, which under basal conditions promoted a repressed chromatin state at RelA target genes through GLP-mediated methylation of histone H3 Lys9 (H3K9). NF-κB-activation–linked phosphorylation of RelA at Ser311 by protein kinase C-ζ (PKC-ζ) blocked the binding of GLP to RelAK310me1 and relieved repression of the target gene. Our findings establish a previously uncharacterized mechanism by which chromatin signaling regulates inflammation programs.

Chromatin dynamics regulate key cellular functions that influence survival, growth and proliferation, and disruption of chromatin homeostasis has been linked to diverse pathologic processes[1]. Methylation of lysine residues of histone, which is catalyzed by protein lysine methyltransferases (PKMTs), is a principal chromatin-regulatory mechanism involved in directing fundamental DNA-templated processes such as transcription and DNA repair[1]. Histone methylation plays a central part in orchestrating proper programming of the genome in response to various stimuli, and aberrant signaling via lysine methylation has been linked to the initiation and progression of many human diseases[2]. Many non-histone proteins are also regulated by lysine methylation, which indicates that this modification is probably a common mechanism for the modulation of protein-protein interactions and signaling pathways[3].

NF-κB is a transcription factor and key inducer of inflammatory responses[4,5]. One of the principal subunits of NF-κB is RelA (p65 (A001645)), which forms either a homodimer or a heterodimer with the structurally related p50 protein (A002937). Under basal conditions, most RelA is sequestered in the cytoplasm because of its association with members of the inhibitor of NF-κB family of proteins[4,5]. Stimulation of cells with NF-κB-activating ligands such as the cytokine tumor necrosis factor (TNF) results in degradation of these inhibitors of NF-κB and translocation of the released NF-κB to the nucleus, where it directs various transcriptional programs[5,6]. In addition to that canonical pathway, there are several additional mechanisms that regulate and fine-tune NF-κB signaling and activation of target genes[7]. For example, various post-translational modifications of RelA influence the specificity, transcriptional activity and activation kinetics of RelA target genes. Furthermore, even in resting conditions, a population of RelA is present in the nucleus, bound at chromatin; however, the functional relevance of this constitutively nuclear population is not known.

Deregulation of NF-κB signaling is linked to many human diseases, including cancer and autoimmune disorders[8]. Thus, understanding the full range of molecular mechanisms that modulate this factor in response to diverse conditions has important biological and clinical implications. Here we screened over 40 known and candidate human PKMTs for methylation of RelA *in vitro*. We identify SETD6 (SET domain–containing protein 6) as a PKMT that monomethylated RelA at Lys310 (RelAK310me1). The ankryin repeat of the PKMT

[1]Department of Biology, Stanford University, Stanford, California, USA. [2]Department of Biochemistry, Emory University School of Medicine, Atlanta, Georgia, USA. [3]Laboratory of Lymphocyte Signaling, The Rockefeller University, New York, New York, USA. [4]EpiNova DPU, Immuno-Inflammation group, GlaxoSmithKline, Stevenage, UK. [5]Department of Carcinogenesis, M.D. Anderson Cancer Center, Smithville, Texas, USA. [6]Department of Molecular Biology, Princeton University, Princeton, New Jersey, USA. [7]Department of Medicine, Division of Immunology and Rheumatology, Stanford University School of Medicine, Stanford, California, USA. [8]Department of Endocrinology, Gerontology, and Metabolism Medicine, Stanford University School of Medicine, Stanford, California, USA. [9]Center for Cancer Epigenetics, University of Texas M.D. Anderson, Houston, Texas, USA. [10]Geriatric Research, Education, and Clinical Center, VA Palo Alto Health Care System, Palo Alto, California, USA. Correspondence should be addressed to O.G. (ogozani@stanford.edu).

Received 15 October; accepted 9 November; published online 5 December 2010; doi:10.1038/ni.1968

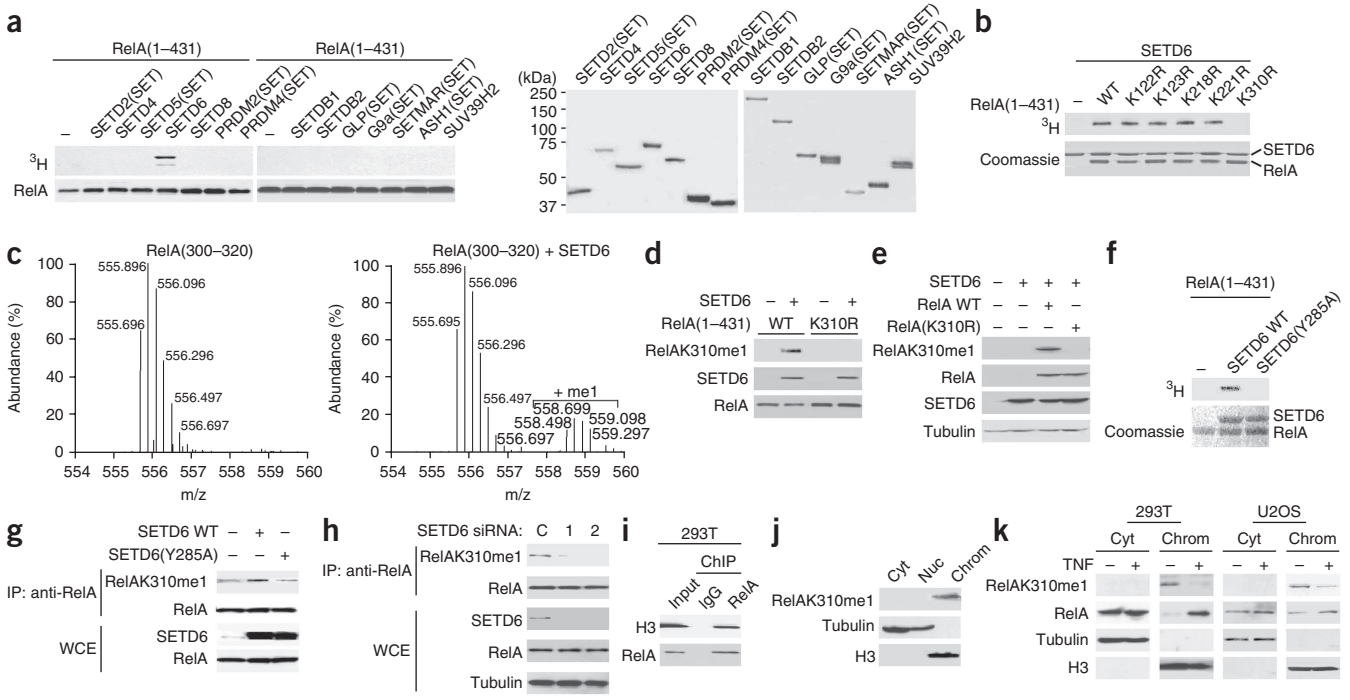

Figure 1 SETD6 monomethylates RelA at Lys310. (**a**) Methylation reactions (^{3}H autoradiogram; left) with recombinant RelA(1–431) as substrate and recombinant PKMT enzymes (full-length or SET domains only; above lanes) and Coomassie staining (right) of recombinant enzymes (left margin, molecular size in kilodaltons (kDa)). Top band, automethylated SETD6. (**b**) SETD6-catalyzed methylation assay (autoradiogram; top) with wild-type or mutant RelA(1–431) (above lanes), and Coomassie staining (below) of proteins used. (**c**) Mass spectrometry analysis of methylation assays of RelA peptide (amino acids 300–320; RelA(300–320)) with (right) or without (left) SETD6; results are presented relative to those of the most abundant ion, set as 100%. Numbers above peaks indicate the mass/charge (m/z) ratio. (**d**) Immunoblot analysis of methylation reactions with (+) or without (–) SETD6 on wild-type (WT) RelA(1–431) or RelA(1–431) with the K310R substitution. (**e**) Immunoblot analysis of whole-cell extracts (WCE; 5% of total) of 293T cells transfected with Flag-tagged SETD6 and either RelA or RelA(K310R), probed with antibodies to various molecules (left margin). (**f**) *In vitro* methylation reaction (top) with wild-type SETD6 or SETD6(Y285A) on RelA(1–431) and Coomassie staining (below) of recombinant proteins used. (**g**) Immunoblot analysis of immunoprecipitated RelA (IP) or WCE (5% of total) from 293T cells transfected with wild-type SETD6 or SETD6(Y285A). (**h**) Immunoblot analysis (as in **g**) of 293T cells treated with control (C) or SETD6-specific siRNA (two independent siRNAs: 1 and 2). (**i**) Immunoblot analysis of RelA or control immunoglobulin G (IgG) protein-protein ChIP, probed with antibodies to various molecules (left margin). Input, 5% of total. (**j**) Immunoblot analysis of 293T cells biochemically separated into cytoplasmic (Cyt), nucleoplasmic (Nuc) or chromatin-enriched (Chrom) fractions; tubulin and H3 signals serve as controls for fractionation integrity. (**k**) Immunoblot analysis of cytoplasmic and chromatin-enriched fractions (as in **j**) from 293T and U2OS cells with (+) or without (–) treatment with TNF (10 ng/ml for 1 h). Data are representative of three (**a**,**b**,**e**,**g**,**h**) or two (**c**,**d**,**f**,**i**–**k**) independent experiments.

GLP (G9A-like protein) functioned as a recognition module for RelAK310me1, which links this mark to localized methylation of histone H3 Lys9 (H3K9) and repressed chromatin at RelAK310me1-occupied genes[9,10]. The SETD6-initiated lysine-methylation signaling cascade acted to restrain activation of NF-κB-mediated inflammatory responses in diverse cell types. This repressive pathway was terminated by phosphorylation of RelA at Ser311 by the atypical protein kinase PKC-ζ (A001934)[11], which blocked recognition of RelAK310me1 by GLP to promote the expression of target genes of RelA. Together our findings identify SETD6 as a previously uncharacterized regulator of the NF-κB network, identify the ankryin-repeat domain of GLP as an effector of methylated RelA, describe a metazoan example of a methylation-phosphorylation switch on a non-histone proteins, and demonstrate a new paradigm for how integrated crosstalk between modifications on transcription factors and histones modulates key physiological and pathological programs.

RESULTS

Monomethylation of RelA at Lys310 by SETD6

To identify additional activities for predicted PKMT enzymes and lysine-methylation events, we screened most of the SET domain–containing proteins present in the human proteome for *in vitro* catalytic activity on various histone and non-histone candidate substrates (**Supplementary Table 1** and data not shown). SETD6, a previously uncharacterized PKMT, methylated an N-terminal RelA polypeptide encompassing amino acids 1-431 (RelA(1–431)) but not a C-terminal polypeptide (residues 430–531; **Fig. 1a** and **Supplementary Fig. 1a**,**b**). Substitution of individual lysine residues with arginine in RelA(1–431) identified Lys310 as the target site of SETD6 (**Fig. 1b**). In contrast, SET7-SET9, which methylates RelA at several lysine residues[12,13], was active on the RelA mutant with replacement of lysine with arginine at position 310 (RelA(K310R); **Supplementary Fig. 1c**). Mass-spectrometry analysis of SETD6-catalyzed methylation of RelA peptides spanning Lys310 (amino acids 300–320) demonstrated that SETD6 added only a single methyl moiety to RelA at Lys310 (**Fig. 1c** and **Supplementary Fig. 2**).

We raised antibodies to SETD6 (**Supplementary Fig. 3**) and the RelAK310me1 epitope (anti-RelAK310me1). Anti-RelAK310me1 specifically recognized RelAK310me1 peptides and did not detect unmodified RelA, RelA dimethylated or trimthrylated at Lys310, or numerous methylated histone peptides (**Supplementary Fig. 4**). Furthermore, anti-RelAK310me1 detected RelA(1–431) that had been methylated *in vitro* by SETD6 but failed to detect unmethylated RelA(1–431) or RelA(K310R) (**Fig. 1d**).

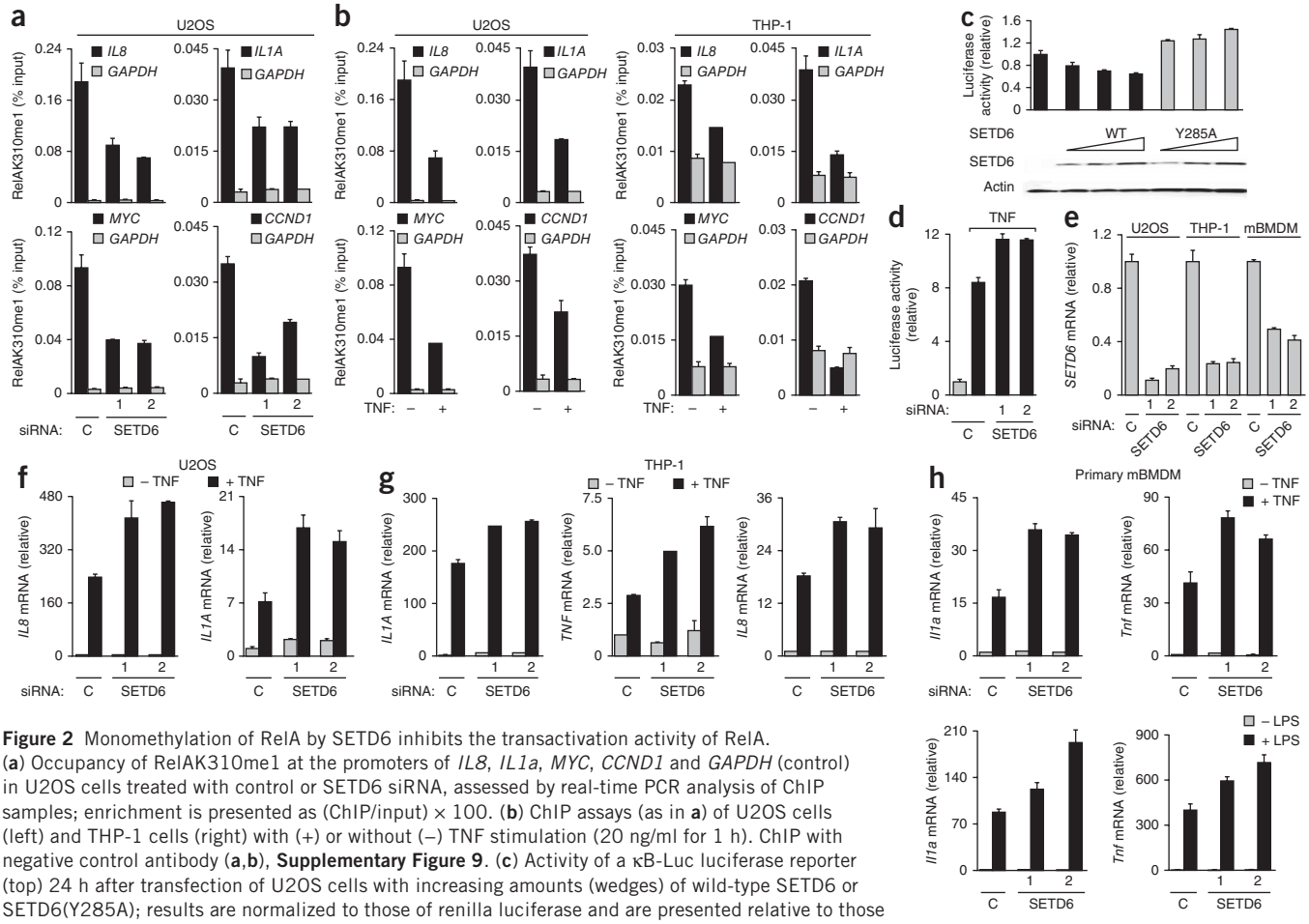

Figure 2 Monomethylation of RelA by SETD6 inhibits the transactivation activity of RelA. (**a**) Occupancy of RelAK310me1 at the promoters of *IL8*, *IL1a*, *MYC*, *CCND1* and *GAPDH* (control) in U2OS cells treated with control or SETD6 siRNA, assessed by real-time PCR analysis of ChIP samples; enrichment is presented as (ChIP/input) × 100. (**b**) ChIP assays (as in **a**) of U2OS cells (left) and THP-1 cells (right) with (+) or without (–) TNF stimulation (20 ng/ml for 1 h). ChIP with negative control antibody (**a**,**b**), **Supplementary Figure 9**. (**c**) Activity of a κB-Luc luciferase reporter (top) 24 h after transfection of U2OS cells with increasing amounts (wedges) of wild-type SETD6 or SETD6(Y285A); results are normalized to those of renilla luciferase and are presented relative to those of cells transfected with control vector. Below, immunoblot analysis of SETD6 and SETD6(Y285A). (**d**) Luciferase activity (as in **c**) in 293T cells transfected with control or SETD6-specific siRNA with (right) or without (far left) TNF treatment (10 ng/ml for 1 h). (**e**) Real-time PCR analysis of the efficiency of knockdown of *SETD6* mRNA by SETD6-specific siRNA in U2OS cells, THP-1 cells and mouse BMDMs (mBMDM), presented relative to its expression in cells transfected with control siRNA (C). (**f**–**h**) Real-time PCR analysis of various mRNAs (vertical axes) in U2OS cells (**f**), THP-1 cells (**g**) and primary mouse BMDMs (**h**) transfected with control or SETD6-specific siRNA with or without TNF (20 ng/ml for 1 h) or LPS (100 ng/ml for 1 h). Data are from at least three experiments (error bars, s.e.m.).

In cotransfection experiments, wild-type RelA was monomethylated by overexpressed SETD6, but RelA(K310R) was not (**Fig. 1e**). Structure-based homology modeling indicated that SETD6 was most similar to the plant enzyme LSMT (Rubisco large subunit methyltransferase)[14] (**Supplementary Fig. 5**). On the basis of that homology, we identified SETD6 with replacement of tyrosine with alanine at position 285 (SETD6(Y285A)) as a catalytic SETD6 mutant *in vitro* (**Fig. 1f** and **Supplementary Figs. 5** and **6**) and found that overexpression of SETD6 led to more monomethylation of endogenous RelA at Lys310, but overexpression of SETD6(Y285A) did not (**Fig. 1g**). Finally, depletion of endogenous SETD6 protein in 293T cells by RNA-mediated interference (RNAi) with two independent small interfering RNAs (siRNAs) resulted in less endogenous RelAK310me1 (**Fig. 1h**). On the basis of these data, we conclude that SETD6 monomethylates RelA at Lys310 *in vitro* and is required for maintenance of physiological concentrations of RelAK310me1 in cells.

Chromatin association of RelAK310me1 under basal conditions

In unstimulated cells, most RelA is localized to the cytoplasm, but a population of RelA is present in the nucleus[15]. In this context, protein-protein chromatin-immunoprecipitation (ChIP) assays in the absence of stimulation demonstrated association of RelA with histone H3 (**Fig. 1i**). Moreover, we detected RelA by ChIP at the promoters of several target genes in unstimulated cells of many types (**Supplementary Fig. 7**). SETD6 was also present in the nucleus (**Supplementary Fig. 3b**). RelA and SETD6 interacted *in vitro* and were coimmunoprecipitated from cells (**Supplementary Fig. 8a–d**). Thus, we reasoned that in contrast to most of RelA, which is localized to the cytoplasm in unstimulated cells[4], the population of RelA that is monomethylated at Lys310 might reside and function in the nucleus. In support of our hypothesis, RelAK310me1 was biochemically fractionated almost exclusively with chromatin in unstimulated 293T human embryonic kidney cells and U2OS human osteosarcoma cells (**Fig. 1j**,**k**). Treatment with TNF, which activates NF-κB[4], resulted in much less RelAK310me1 at chromatin than did no stimulation (**Fig. 1k**). On the basis of these data, we conclude that RelAK310me1 is present at chromatin in unstimulated cells.

Next we did ChIP assays with U2OS cells under basal conditions to determine if RelAK310me1 is bound to chromatin at the promoters of RelA target gene. RelAK310me1 occupied the promoters of several RelA target genes (*IL8*, *IL1A*, *MYC* and *CCND1*), and detection of this RelA species at target promoters was lost in U2OS cells treated with either of two independent siRNAs targeting SETD6 (**Fig. 2a** and **Supplementary Fig. 9a**), as well as in U2OS cells stably expressing a short hairpin RNA

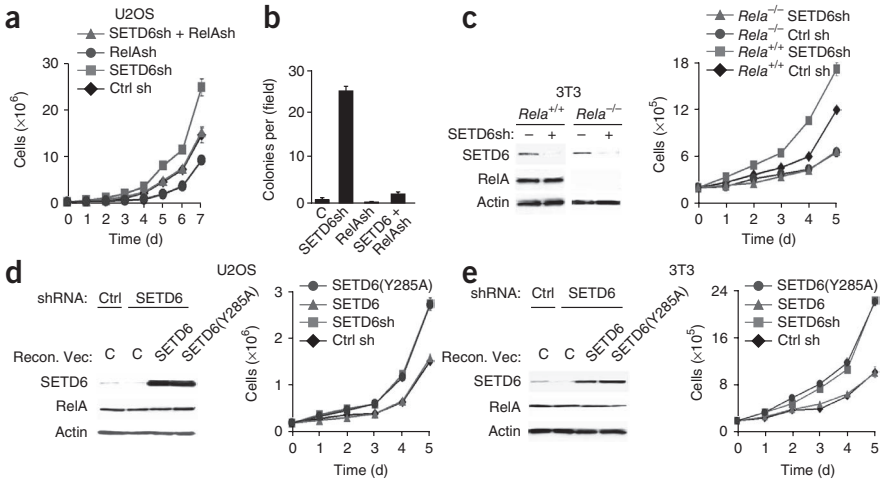

Figure 3 SETD6 attenuates RelA-driven cell proliferation. (**a**) Growth of U2OS cells treated with control shRNA (Ctrl sh) or SETD6-specific shRNA (SETD6sh) and/or RelA-specific shRNA (RelAsh), assessed daily for 7 d. (**b**) Colonies of U2OS cells, treated as in **a**, in soft agar. (**c**) Growth of *Rela*$^{+/+}$ and *Rela*$^{-/-}$ MEFs treated and assessed as in **a** (right), and immunoblot analysis of WCE of *Rela*$^{+/+}$ and *Rela*$^{-/-}$ 3T3 fibroblasts left untreated (–) or treated with SETD6-specific shRNA (+). (**d**,**e**) Growth curves (right) and immunoblot analysis (of WCE; left) of U2OS cells (**d**) and 3T3 fibroblasts (**e**) treated with control or SETD6-specific shRNA and reconstituted (Recon vec) with SETD6 or SETD6(Y285A) or not reconstituted (C). Data are from at least three independent experiments (error bars, s.e.m.).

(shRNA) targeting SETD6 (**Supplementary Fig. 10**). Consistent with the results obtained with the cellular fractionation assays (**Fig. 1j**,**k**), treatment with TNF resulted in less occupancy by RelAK310me1 at promoters of target genes both in U2OS cells and in the THP-1 acute monocytic leukemia cell line (**Fig. 2b** and **Supplementary Fig. 9b**). Thus, monomethylation of RelAK310 is a chromatin-associated modification and is inversely correlated with activation of NF-κB by TNF.

SETD6 attenuates transcription of RelA target genes

To investigate the relationship between SETD6 and the transcriptional activity of RelA, we cotransfected U2OS cells with an NF-κB-driven reporter[16] and either SETD6 or SETD6(Y285A). The activity of this reporter was repressed by SETD6 in a dose-dependent manner and required that the catalytic activity of SETD6 be intact (**Fig. 2c**). In addition, depletion of SETD6 resulted in more reporter activity in unstimulated cells (**Supplementary Fig. 11**) and after exposure to TNF (**Fig. 2d**). These data suggested that SETD6 represses physiological transactivation by RelA. To test that hypothesis, we depleted U2OS cells, THP-1 cells and primary mouse bone marrow–derived macrophages (BMDMs) of SETD6 (**Fig. 2e**) and measured mRNA for canonical NF-κB targets in the presence or absence of NF-κB stimulation[4] (**Fig. 2f–h**). In response to TNF, knockdown of SETD6 led to more expression of RelA target genes than their expression in control cells for all three cell types (**Fig. 2f–h**). We obtained similar results with mouse BMDMs stimulated with lipopolysaccharide (LPS; **Fig. 2h**, right). In addition, depletion of SETD6 resulted in higher basal expression of a subset of RelA target genes (**Supplementary Fig. 12**). We noted that SETD6 did not methylate the RelA partner p50 (**Supplementary Fig. 1d**) and, in contrast to known histone lysine methyltransferases such as G9a and GLP[9,17], SETD6 did not methylate nucleosomes (**Supplementary Fig. 1e**). Finally, genome-wide gene-expression analysis of *Rela*$^{-/-}$ mouse embryonic fibroblasts (MEFs)[18] reconstituted with wild-type mouse RelA or mutant mouse RelA(K310R) showed that in the absence of stimulation, cells complemented with RelA(K310R) expressed more RelA-regulated genes and expression of these genes was higher than that of cells complemented with wild-type RelA (**Supplementary Fig. 13** and **Supplementary Data**), which indicated involvement of Lys310 in regulating the expression of RelA target genes. Together these results indicate that SETD6-mediated methylation of RelAK310 has an inhibitory effect on expression of many RelA-regulated genes.

Attenuation of RelA-driven inflammatory responses by SETD6

Hyperactive NF-κB has been linked to the development and progression of many types of cancer[8]. To investigate potential roles for SETD6 and the interaction of SETD6 and RelA in cellular transformation, we established U2OS cells with stable expression of shRNAs targeting SETD6 alone, RelA alone or SETD6 and RelA, or a control shRNA, and assessed cell transformation–associated properties (**Fig. 3a**,**b** and **Supplementary Fig. 14**). Knockdown of SETD6 accelerated the proliferation rate of cells in a RelA-dependent way relative to the proliferation of control cells (**Fig. 3a**). In addition, depletion of SETD6 conferred a 25-fold greater ability of cells to form colonies in soft agar than that of control cells or cells depleted of RelA, and depletion of both RelA and SETD6 reversed the anchorage-independent growth advantage provided by knockdown of SETD6 alone (**Fig. 3b**). Depletion of SETD6 also led to higher cell proliferation rates in wild-type 3T3 mouse embryonic fibroblasts but not in *Rela*$^{-/-}$ 3T3 cells (**Fig. 3c**). Next, we depleted human U2OS cells and mouse 3T3 cells of endogenous SETD6 through the use of shRNA targeting the 3′ untranslated region of human or mouse SETD6, respectively (**Fig. 3d**,**e**). We reconstituted the cells depleted of SETD6 with exogenous SETD6 or exogenous SETD6(Y285A) that lacked the 3′ untranslated region and was therefore resistant to shRNA. Complementation with wild-type SETD6 reestablished a normal proliferative rate, whereas complementation with SETD6(Y285A) failed to do so (**Fig. 3d**,**e**). These data suggest that the enzymatic activity of SETD6 regulates a RelA-dependent effect on cell proliferation.

In addition to being linked to cancer, NF-κB—as a key regulator of inflammation—has also been linked to the etiology of inflammatory and autoimmune diseases[5,8]. Analysis of published gene-expression data sets comparing peripheral blood mononuclear cells from patients suffering from rheumatoid arthritis, septic shock or juvenile idiopathic arthritis with control samples showed downregulation of *SETD6* mRNA in the disease state (**Fig. 4a** and **Supplementary Fig. 15**). In addition, SETD6 expression was lower in patients with rheumatoid arthritis who responded to TNF inhibitors than in patients who were not responsive to this treatment (**Supplementary Fig. 15b**), which suggested a role for NF-κB in their rheumatoid arthritis disease.

The inverse correlation between SETD6 expression and NF-κB-linked inflammatory diseases and the observation that SETD6 attenuates RelA-dependent transactivation of cytokines such as interleukin 1α (IL-1α) and TNF suggest that SETD6 might have a role in mitigating NF-κB-driven inflammatory responses. Consistent with a negative role for SETD6 in NF-κB signaling, in monocytic THP-1 cells exposed to TNF, knockdown of SETD6 led to more production of the secreted cytokines TNF and IL-6 than that of cells treated with control siRNA

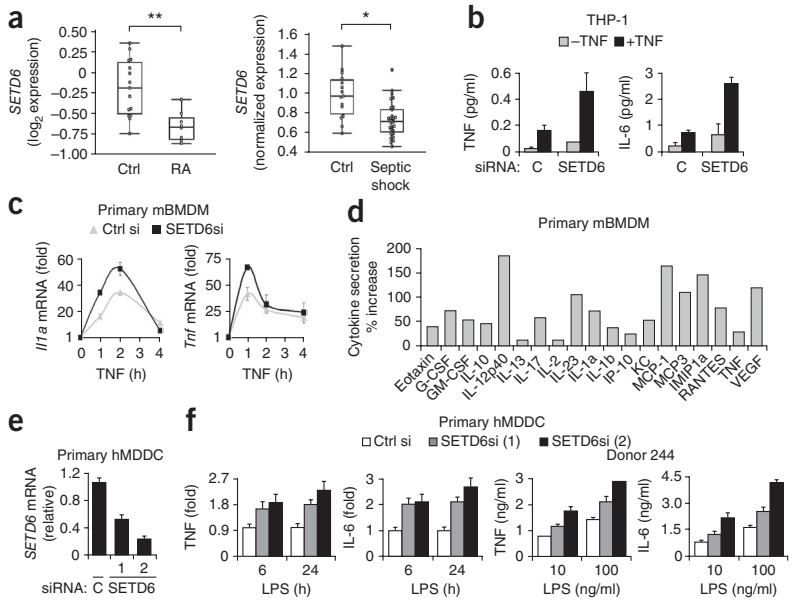

Figure 4 SETD6 attenuates RelA-driven inflammatory responses. (**a**) *SETD6* expression in patients with rheumatoid arthritis (RA; $n = 8$) and healthy controls ($n = 15$), presented as the normalized $\log_2$ ratio of the sample compared with a common reference (left); and *SETD6* expression in patients with septic shock ($n = 30$) and healthy controls ($n = 15$), presented relative to the median of the results obtained with healthy controls (right). Each symbol (in boxes) represents an individual sample. $^*P = 0.0015$ and $^{**}P = 0.00036$ (two-tailed *t*-test). (**b**) Enzyme-linked immunosorbent assay of cytokines in supernatants of THP-1 cells transfected with control siRNA or SETD6-specific siRNA with or without TNF (20 ng/ml). (**c**) Real-time PCR analysis of *Il1a* and *Tnf* mRNA in mouse BMDMs transfected with control siRNA (Ctrl si) or SETD6-specific siRNA (SETD6si). (**d**) Multiplex enzyme-linked immunosorbent assay of RelA-regulated cytokines in supernatants of primary mouse BMDMs treated for 2 h as in **c**, presented as (SETD6 siRNA / control siRNA – 1) × 100. (**e**) Real-time PCR analysis of *SETD6* mRNA in primary human monocyte-derived dendritic cells (hMDDC; $n = 3$ donors) transfected with control siRNA (C) or SETD6-specific siRNA (1,2). (**f**) Secretion of TNF and IL-6 by human monocyte-derived dendritic cells transduced with siRNA as in **e** and treated for 6 or 24 h with LPS (left; $n = 3$ donors) or at 24 h after treatment with 10 or 100 ng/ml of LPS (right; $n = 1$ donor). Data are an analysis of published studies (**a**; error bars indicate minimum and maximum values within 1.5 interquartile range of the lower and upper quartile, respectively), are from at least three independent experiments (**b**,**c**,**e**,**f**; error bars, s.e.m.) or are representative of two independent experiments (**d**).

(**Fig. 4b**). We next assessed the relationship between SETD6 depletion and cytokine production in mouse BMDMs. First, kinetic analysis showed that in response to TNF and LPS, the abundance of *Il1a* and *Tnf* mRNA was higher in cells depleted of SETD6 than in control cells across a range of time points (**Fig. 4c** and **Supplementary Fig. 16a**; SETD6-knockdown efficiency; **Fig. 2e**). Furthermore, multiplex cytokine analysis of supernatants of these cells demonstrated upregulation of nearly 20 secreted NF-κB-regulated cytokines in cells depleted of SETD6 relative to their expression in control cells in response to TNF (**Fig. 4d**) and LPS (**Supplementary Fig. 16b**). Finally, depletion of SETD6 with two independent siRNAs in primary monocyte-derived dendritic cells isolated from human donors (**Fig. 4e**) conferred a

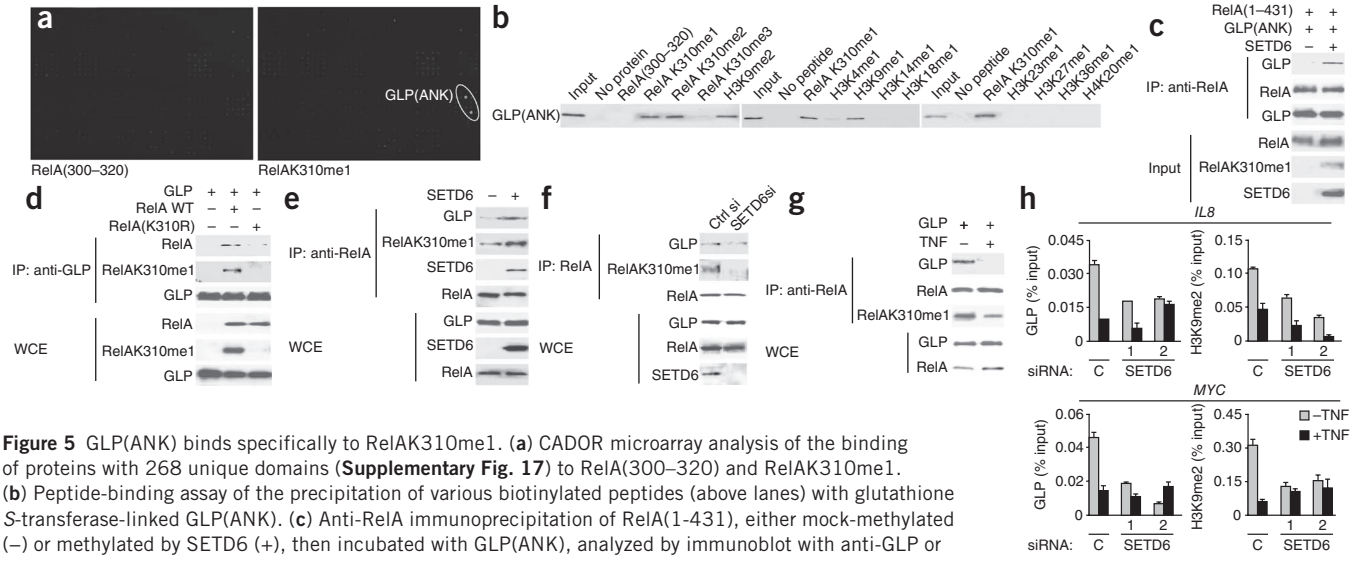

Figure 5 GLP(ANK) binds specifically to RelAK310me1. (**a**) CADOR microarray analysis of the binding of proteins with 268 unique domains (**Supplementary Fig. 17**) to RelA(300–320) and RelAK310me1. (**b**) Peptide-binding assay of the precipitation of various biotinylated peptides (above lanes) with glutathione *S*-transferase-linked GLP(ANK). (**c**) Anti-RelA immunoprecipitation of RelA(1-431), either mock-methylated (–) or methylated by SETD6 (+), then incubated with GLP(ANK), analyzed by immunoblot with anti-GLP or anti-RelA. Below, immunoblot analysis of input (10% of starting material). (**d**) Immunoprecipitation (with anti-Flag) of proteins from 293T cells transfected with plasmids encoding Flag-tagged GLP and wild-type RelA or RelA(K310R), followed by immunoblot analysis of immunoprecipitates and WCE (10% of total). (**e**) Immunoprecipitation (with anti-RelA) of proteins from 293T cells left untransfected (–) or transfected with plasmid encoding SETD6, followed by immunoblot analysis of immunoprecipitates and WCE (10% of total). (**f**) Immunoprecipitation and immunoblot analysis as in **e** of 293T cells treated with control or SETD6-specific siRNA. (**g**) Immunoprecipitation and immunoblot analysis as in **e** of U2OS cells transfected with plasmid encoding GLP, with or without TNF treatment (10 ng/ml). (**h**) Occupancy of GLP and H3K9me2 at the *IL8* and *MYC* promoters in U2OS cells treated with control siRNA (C) or SETD6-specific siRNA (1,2), with or without TNF treatment (20 ng/ml), assessed as in **Figure 2a** (ChIP with negative control antibody, **Supplementary Fig. 19**). Data are representative of three (**a**,**b**) or two (**c**–**g**) independent experiments or are from at least three experiments (**h**; error bars, s.e.m.).

Table 1 Binding affinity of GLP(ANK)

Peptide	Ligand	K_d (μm)
RelA(300–320)	GLP	NB
RelAK310me1	GLP	4.8 ± 0.4
RelAK310me2	GLP	5.4 ± 0.5
RelAK310me3	GLP	NB
RelAK310me1S311ph	GLP	NB
H3K9me1	GLP	5.0 ± 0.3

Isothermal titration calorimetry analysis of the affinity of the binding of GLP(ANK) to various peptides (left column), presented as the dissociation constant (K_d). NB, no binding. RelAK310me2 and RelAK310me3, RelA di- and trimethylated, respectively, at Lys310; RelAK310me1S311ph, RelAK310me1 with phosphorylation of Ser311. Data are representative of three independent experiments (mean ± s.e.m.).

time- and dose-dependent increase in secretion of the cytokines TNF and IL-6 in response to LPS stimulation (**Fig. 4f**). Together these experiments indicate that SETD6 inhibits the production of a broad array of NF-κB-regulated cytokines in diverse cell types, including antigen-presenting cells, which suggests that SETD6 is a critical repressor of RelA-mediated inflammatory responses.

GLP ankyrin repeat is a RelAK310me1 effector domain

To understand the molecular basis of the repressive function associated with RelAK310me1, we screened CADOR microarrays[19] for protein motifs that could potentially act as transducers of this mark (**Supplementary Fig. 17**). Of the 268 proteins on the array, the RelAK310me1 peptide bound specifically to only one: the ankyrin-repeat domain of GLP (GLP(ANK); **Fig. 5a**). Peptide-precipitation assays and measurement of dissociation constants independently confirmed and characterized the interaction between GLP(ANK) and RelAK310me1 (**Fig. 5b** and **Table 1**). These data also demonstrated that except for the positive-control monomethylated and dimethylated H3K9 peptides[20], other methylated histone peptides did not bind to GLP(ANK) (**Fig. 5b**) and that GLP(ANK) had similar binding affinities for RelAK310me1 and monomethylated H3K9 (ref. 20; **Table 1** and **Supplementary Fig. 18**). In addition, GLP(ANK) did not bind nonmethylated or trimethylated RelAK310 peptides (**Fig. 5b** and **Table 1**), which indicated that the recognition of RelAK310 requires mono- or dimethylation. Finally recombinant GLP(ANK) bound recombinant RelA(1–431) in coimmunoprecipitation experiments, but only after RelA(1–431) was methylated *in vitro* by SETD6 (**Fig. 5c**). From these data we conclude that GLP(ANK) binds specifically to RelAK310me1 *in vitro*.

Next we investigated the ability of RelAK310me1 to be recognized by GLP in cells. Exogenous GLP coimmunoprecipitated overexpressed wild-type RelA but not RelA(K310R) (**Fig. 5d** and **Supplementary Fig. 8e**). In addition, SETD6 expression enhanced the interaction between endogenous GLP and RelA (**Fig. 5e**). Decreasing the abundance of RelAK310me1 by depleting SETD6 via RNAi or TNF treatment inhibited the association of GLP with RelA (**Fig. 5f**,**g**). These data suggest that in the absence of NF-κB activation, RelA and GLP directly interact and that this interaction requires SETD6-dependent monomethylation of RelA at Lys310.

GLP and its heterodimeric partner G9a generate mono- and dimethylated H3K9 at euchromatin to repress transcription[9,21], and methylation of H3K9 suppresses the expression of inducible inflammatory genes[10]. Our observations that methylation of RelA by SETD6 inhibited the expression of NF-κB target genes and that GLP bound to RelAK310me1 suggested a model in which the content of histone H3 dimethylated at Lys9 (H3K9me2) is greater at RelAK310me1-occupied NF-κB target genes in unstimulated cells because of the stabilization of GLP through its interaction with RelAK310me1. Two predictions of this model are as follows: first, under basal conditions and in a SETD6-dependent manner, the chromatin of distinct RelA-regulated gene promoters should be enriched for GLP and H3K9me2; and second, GLP should be required for SETD6 to inhibit expression of these RelA-regulated genes. In support of the first prediction, ChIP assays demonstrated less occupancy by GLP and H3K9me2 at the promoters of *IL8* and *MYC* in response to TNF stimulation (**Fig. 5h** and **Supplementary Fig. 19**), and knockdown of SETD6 with two independent siRNAs largely eliminated the baseline enrichment of GLP and H3K9me2 at these promoters (**Fig. 5h** and **Supplementary Fig. 19**). We obtained similar results with cells stably depleted of SETD6 by an shRNA approach (**Supplementary Fig. 20**). In addition, induction of RelAK310me1 via SETD6 overexpression resulted in more occupancy by GLP and H3K9me2 at two RelA target promoters (**Supplementary Fig. 21a**). Thus, these data demonstrate a role for SETD6 and RelAK310me1 in stabilizing GLP activity at specific RelA target genes.

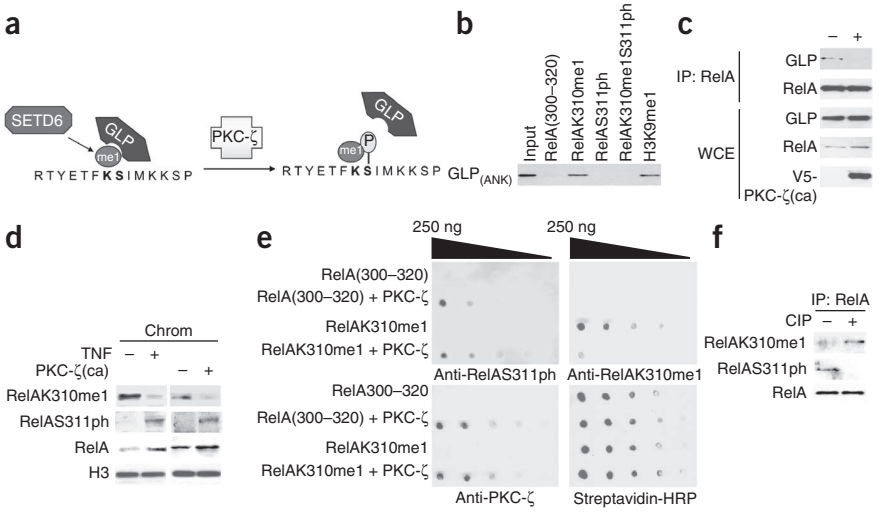

Figure 6 Phosphorylation of RelA at S311 by PKC-ζ blocks GLP recognition of RelAK310me1. (**a**) Model of the mechanism by which a methylation-phosphorylation switch at RelA Lys310 and Ser311 (bolded residues) regulates the recognition of RelAK310me1 by GLP. (**b**) Peptide-binding assay of the precipitation of various biotinylated peptides (above lanes) with glutathione *S*-transferase–linked GLP(ANK). (**c**) Immunoprecipitation (with anti-RelA) of proteins from 293T cells left untransfected (–) or transfected with plasmid encoding PKC-ζ(ca), followed by immunoblot analysis of immunoprecipitates and WCE (5% of total). Bottom row, blot probed antibody to V5-tagged PKC-ζ(ca). (**d**) Immunoblot analysis of chromatin-enriched fractions (Chrom) isolated from 293T cells with or without treatment with TNF or transfection of V5-tagged PKC-ζ(ca) (above lanes). (**e**) Dot-blot analysis of *in vitro* kinase reactions with recombinant PKC-ζ plus various peptides (left margin), spotted at a concentration of 0.25 μg/μl followed by 5× serial dilutions (wedges), probed with anti-RelAS311ph, anti-RelAK310me1, anti-PKC-ζ or horseradish peroxidase (HRP)-conjugated streptavidin (loading control). (**f**) Immunoblot analysis of RelA immunoprecipitated from 293T cells transfected with V5-tagged PKC-ζ(ca) and left untreated (–) or treated for 1 h (+) with calf intestinal alkaline phosphatase (CIP). Data are representative of two (**b**,**c**,**e**,**f**) or three (**d**) independent experiments.

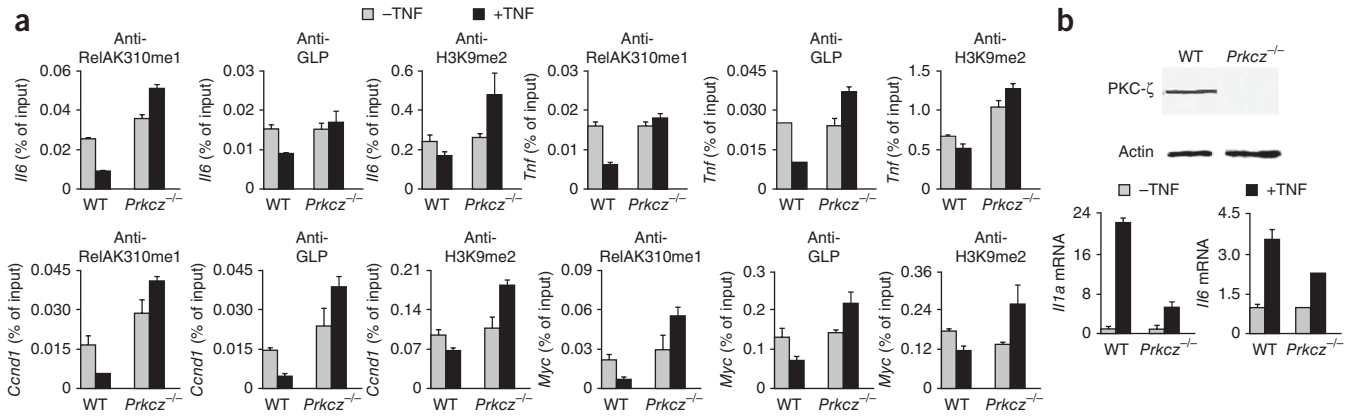

Figure 7 RelA methylation-phosphorylation switch at chromatin regulates NF-κB signaling. (**a**) ChIP assay of RelAK310me1, GLP and H3K9me2 at the promoters of *Il6*, *Tnf*, *Ccnd1* and *Myc* in *Prkcz*$^{+/+}$ (WT) and *Prkcz*$^{-/-}$ MEFs[23] with or without TNF treatment (20 ng/ml), presented as in **Figure 2a** (ChIP with negative control antibody, **Supplementary Fig. 24**). (**b**) Real-time PCR analysis (below) of *Il1a* and *Il6* mRNA in *Prkcz*$^{+/+}$ and *Prkcz*$^{-/-}$ cells with or without TNF treatment (20 ng/ml), and immunoblot analysis (above) of PKC-ζ in *Prkcz*$^{+/+}$ and *Prkcz*$^{-/-}$ MEFs[23]. Data are from at least three experiments (error bars, s.e.m.).

To investigate the functional interaction between GLP and SETD6-mediated attenuation of RelA transcriptional activity, we depleted cells of GLP and challenged them with TNF and found they had more *IL8* and *MYC* mRNA than did cells treated with control shRNA (**Supplementary Fig. 22a**). Moreover, the ability of SETD6 overexpression to suppress baseline expression of *IL8* and *MYC* mRNA was largely abrogated in cells depleted of GLP (**Supplementary Fig. 22b**). These data indicate that inhibition of NF-κB signaling by SETD6 occurs at chromatin and is mediated by a lysine-methylation network that connects SETD6 activity on RelA to GLP activity on H3K9.

RelA phosphorylation blocks GLP-RelAK310me1 interaction

TNF stimulation initiates several activating phosphorylation events on RelA[7], including phosphorylation at Ser311 by the atypical protein kinase PKC-ζ[11]. The molecular mechanism by which phosphorylation of Ser311 activates RelA is not known[11]. Because methylation of Lys310 and phosphorylation of Ser311 are coupled to opposing biological outcomes and the two modifications are in close physical proximity, we postulated that phosphorylation of Ser311 functionally inhibited the recognition of RelAK310me1 by GLP (**Fig. 6a**). The ability of GLP(ANK) to bind RelAK310me1 peptides was abolished when Ser311 was phosphorylated, as determined by isothermal titration calorimetry (**Table 1**) and peptide-precipitation assays (**Fig. 6b**). Moreover, overexpression of constitutively active V5-tagged PKC-ζ (PKC-ζ(ca))[22] disrupted the endogenous interaction between RelA and GLP (**Fig. 6c**). Consistent with the idea of a physiological role for RelA phosphorylated at S311 (RelAS311ph) in regulating the binding of GLP to RelA at chromatin, treatment with TNF (and overexpression of V5-tagged PKC-ζ(ca)) resulted in a stronger RelAS311ph signal at chromatin, but a weaker RelAK310me1 signal (**Fig. 6d**). Thus, we propose that phosphorylation of Ser311 masks RelAK310me1 to prevent its recognition by GLP(ANK) (**Fig. 6a**).

Antibody to the RelAS311ph epitope recognized the RelAS311ph mark regardless of methylation at Lys310 (**Supplementary Fig. 23**). In contrast, recognition of RelAK310me1 by anti-RelAK310me1 was disrupted by phosphorylation of Ser311, as observed in dot-blot assays with a dually modified peptide containing monomethylation of Lys310 and phosphorylation of Ser311 (**Supplementary Fig. 23b**) or with a RelAK310me1 peptide phosphorylated at Ser311 *in vitro* by recombinant PKC-ζ (**Fig. 6e**). These results also demonstrate that PKC-ζ phosphorylated Ser311 regardless of the monomethylation status of Lys310 (**Fig. 6e**). Furthermore, detection of endogenous RelAK310me1 on RelA immunoprecipitated from cells overexpressing V5-tagged PKC-ζ(ca) was much greater after *in vitro* dephosphorylation of the immunoprecipitated protein (**Fig. 6f** and **Supplementary Fig. 23c**), which indicated that the RelAK310me1 epitope becomes exposed after removal of RelAS311ph and therefore demonstrated that the two marks probably co-occupy the same molecule. Together these findings suggest that TNF-induced phosphorylation of chromatin-bound RelAK310me1 at Ser311 disrupts the association of GLP with RelA, thereby promoting activation of the population of NF-κB target genes occupied by RelAK310me1.

A RelA methylation-phosphorylation switch in NF-κB signaling

Consistent with the hypothesis outlined above, coexpression of V5-tagged PKC-ζ(ca) with SETD6 abrogated the greater occupancy of RelA target genes by RelAK310me1, GLP and H3K9me2 induced by SETD6 expression alone (**Supplementary Fig. 21a**). In addition, SETD6 failed to inhibit the expression of *IL8* and *MYC* when coexpressed with PKC-ζ(ca) (**Supplementary Fig. 22b**). Indeed, expression of V5-tagged PKC-ζ(ca) induced more expression of *IL8* and *MYC* above baseline, whereas the ability of V5-tagged PKC-ζ(ca) to antagonize SETD6 and stimulate the activation of RelA target genes was abrogated in cells depleted of GLP (**Supplementary Fig. 22b**). Finally, the occupancy by RelAK310me1, GLP and H3K9me2 at promoters of four different RelA target genes involved in cell proliferation and inflammation was lower after TNF stimulation in PKC-ζ-sufficient MEFs, but we did not observe these changes in PKC-ζ-deficient (*Prkcz*$^{-/-}$) MEFs[23] (**Fig. 7a** and **Supplementary Fig. 24**). In agreement with the ChIP results and as reported before[23], TNF induction of the expression of *Il1a* and *Il6* was largely attenuated in *Prkcz*$^{-/-}$ cells (**Fig. 7b**). These results support a model in which the chromatin environment of NF-κB target genes can be regulated by competing modifications of RelA by SETD6 and PKC-ζ, with the inert state linked to SETD6-mediated binding of GLP to RelAK310me1 and the active state linked to PKC-ζ-mediated disassociation of GLP from RelAK310me because of phosphorylation of Ser311 (**Supplementary Fig. 25**).

DISCUSSION

We have reported here the discovery of a previously unknown lysine-methylation event that occurs on the transcription factor RelA,

which is catalyzed by SETD6 and regulates the clinically important NF-κB pathway. Monomethylation of nuclear RelA at Lys310 by SETD6 attenuated NF-κB signaling by docking GLP (via its ankyrin repeats) at target genes to generate a silent chromatin state, effectively rendering chromatin-bound RelA inert. As deregulation of NF-κB is linked to pathological inflammatory processes and cancer[8] and SETD6 inhibits NF-κB signaling in diverse cell types, including primary human cells, SETD6 provides another link by which methylation of lysine residues of proteins and regulation of chromatin influence tumor suppression and anti-inflammatory responses[2,5].

SET7-SET9 is a well-characterized PKMT with many protein substrates[3], including TNF-dependent methylation of RelA at three different lysine residues[12,13]. In contrast, SETD6 methylated RelA at a single residue (Lys310), and this occurred in the absence of stimulation and was functionally suppressed by TNF-induced phosphorylation of RelA at Ser311. Thus, RelAK310me1 represents a specialized population of RelA that is not sequestered in the cytoplasm under basal conditions but is instead bound and quiescent at target promoters. We postulate that methylation of transcription factors such as RelA can aid in the rapid and dynamic modulation of specific gene-expression programs by establishing transcriptional memory at marked genes[24]. In addition, the SETD6-RelA-GLP-H3K9me2 network delineated here constitutes the first description to our knowledge of a lysine-methylation signaling cascade. We have also demonstrated that TNF-induced phosphorylation of RelA Ser311 terminated SETD6 action by blocking recognition of RelAK310me1 by GLP, which in turn led to chromatin relaxation and expression of RelA target genes. These findings provide the first example to our knowledge of a metazoan regulatory methylation-phosphorylation switch on a non-histone protein[25–27]. Together our results emphasize how the convergence and integration of multiple signals at chromatin can modify important biological and disease pathways.

METHODS

Methods and any associated references are available in the online version of the paper at http://www.nature.com/natureimmunology/.

Accession codes. UCSD-Nature Signaling Gateway (http://www.signaling-gateway.org): A001645, A002937 and A001934.

Note: Supplementary information is available on the Nature Immunology website.

ACKNOWLEDGMENTS

We thank R. Kingston and M. Simon (Harvard Medical School) for recombinant nucleosomes; J. Smith (University of Alabama Birmingham) for the PKC-ζ(ca) plasmid; W.C. Greene (University of California San Francisco) for RelA(1–431) cDNA and the κB-Luc luciferase reporter plasmid; D. Reinberg (New York University) for the NSD1(SET) plasmid; M. Covert (Stanford University) and T.D. Gilmore (Boston University) for the wild-type and *Rela*$^{-/-}$ mouse 3T3 cells; J. Moscat (University of Cincinnati College of Medicine) for the wild-type and *Prkcz*$^{-/-}$ MEFs; E. Engleman (Stanford University) for FL-B16 cells; E. Green for critical reading of the manuscript; and A. Alizadeh for comments. Supported by the National Institutes of Health (DA025800 to O.G. and M.T.B.; GM068680 to X.C.; and F32AI080086 to C.L.L.), the American Society for Mass Spectrometry (B.A.G.), the National Heart, Lung and Blood Institute (HHSN-268201999934C to P.J.U.), the National Institute of Allergy and Infectious Diseases (U19-AI082719 to P.J.U.), the Floren Family Trust (P.J.U.), the Genentech Foundation (A.J.K.), the European Molecular Biology Organization (D.L.), the Human Frontier Science Program (D.L.), the Machiah Foundation (D.L.), the Georgia Research Alliance (X.C.) and the Ellison Medical Foundation (O.G.)

AUTHOR CONTRIBUTIONS

D.L. did most of the molecular biology and cellular studies; Y.C. did binding affinity studies and modeling; A.J.K., P.C. and X.S. generated the PKMT library; A.J.K. identified and initially characterized the activity of SETD6 on RelA Lys310; B.Z. did mass spectrometry analysis; U.S. and C.K. did the primary cells experiments; A.E. did CADOR array experiments; C.L.L. analyzed gene expression data sets; R.I.T., S.T., A.Y.K., R.C. and S.T. provided technical support; X.S., P.J.U., K.C., B.G., R.P., M.B., A.T., X.C. and O.G. discussed studies; D.L. and O.G. designed studies, analyzed data, and wrote the paper; D.L. and A.J.K. contributed independently to the work; and all authors discussed and commented on the manuscript.

COMPETING FINANCIAL INTERESTS

The authors declare competing financial interests: details accompany the full-text HTML version of the paper at http://www.nature.com/natureimmunology/.

Published online at http://www.nature.com/natureimmunology/.
Reprints and permissions information is available online at http://npg.nature.com/reprintsandpermissions/.

1. Kouzarides, T. Chromatin modifications and their function. *Cell* **128**, 693–705 (2007).
2. Albert, M. & Helin, K. Histone methyltransferases in cancer. *Semin. Cell Dev. Biol.* **2**, 209–220 (2009).
3. Huang, J. & Berger, S.L. The emerging field of dynamic lysine methylation of non-histone proteins. *Curr. Opin. Genet. Dev.* **18**, 152–158 (2008).
4. Hoffmann, A., Natoli, G. & Ghosh, G. Transcriptional regulation via the NF-κB signaling module. *Oncogene* **25**, 6706–6716 (2006).
5. Natoli, G. Control of NF-κB-dependent transcriptional responses by chromatin organization. *Cold Spring Harb Perspect Biol* **1**, a000224 (2009).
6. Ghosh, S. & Hayden, M.S. New regulators of NF-κB in inflammation. *Nat. Rev. Immunol.* **8**, 837–848 (2008).
7. Perkins, N.D. Post-translational modifications regulating the activity and function of the nuclear factor κB pathway. *Oncogene* **25**, 6717–6730 (2006).
8. Grivennikov, S.I., Greten, F.R. & Karin, M. Immunity, inflammation, and cancer. *Cell* **140**, 883–899 (2010).
9. Tachibana, M. *et al.* Histone methyltransferases G9a and GLP form heteromeric complexes and are both crucial for methylation of euchromatin at H3–K9. *Genes Dev.* **19**, 815–826 (2005).
10. Saccani, S. & Natoli, G. Dynamic changes in histone H3 Lys 9 methylation occurring at tightly regulated inducible inflammatory genes. *Genes Dev.* **16**, 2219–2224 (2002).
11. Duran, A., Diaz-Meco, M.T. & Moscat, J. Essential role of RelA Ser311 phosphorylation by ζPKC in NF-κB transcriptional activation. *EMBO J.* **22**, 3910–3918 (2003).
12. Ea, C.K. & Baltimore, D. Regulation of NF-κB activity through lysine monomethylation of p65. *Proc. Natl. Acad. Sci. USA* **106**, 18972–18977 (2009).
13. Yang, X.D. *et al.* Negative regulation of NF-κB action by Set9-mediated lysine methylation of the RelA subunit. *EMBO J.* **28**, 1055–1066 (2009).
14. Trievel, R.C., Flynn, E.M., Houtz, R.L. & Hurley, J.H. Mechanism of multiple lysine methylation by the SET domain enzyme Rubisco LSMT. *Nat. Struct. Biol.* **10**, 545–552 (2003).
15. Dong, J., Jimi, E., Zeiss, C., Hayden, M.S. & Ghosh, S. Constitutively active NF-κB triggers systemic TNFα-dependent inflammation and localized TNFα-independent inflammatory disease. *Genes Dev.* **24**, 1709–1717 (2010).
16. Chen, L., Fischle, W., Verdin, E. & Greene, W.C. Duration of nuclear NF-κB action regulated by reversible acetylation. *Science* **293**, 1653–1657 (2001).
17. Tachibana, M., Sugimoto, K., Fukushima, T. & Shinkai, Y. Set domain-containing protein, G9a, is a novel lysine-preferring mammalian histone methyltransferase with hyperactivity and specific selectivity to lysines 9 and 27 of histone H3. *J. Biol. Chem.* **276**, 25309–25317 (2001).
18. Buerki, C. *et al.* Functional relevance of novel p300-mediated lysine 314 and 315 acetylation of RelA/p65. *Nucleic Acids Res.* **36**, 1665–1680 (2008).
19. Kim, J. *et al.* Tudor, MBT and chromo domains gauge the degree of lysine methylation. *EMBO Rep.* **7**, 397–403 (2006).
20. Collins, R.E. *et al.* The ankyrin repeats of G9a and GLP histone methyltransferases are mono- and dimethyllysine binding modules. *Nat. Struct. Mol. Biol.* **15**, 245–250 (2008).
21. Tachibana, M., Matsumura, Y., Fukuda, M., Kimura, H. & Shinkai, Y. G9a/GLP complexes independently mediate H3K9 and DNA methylation to silence transcription. *EMBO J.* **27**, 2681–2690 (2008).
22. Smith, L. *et al.* Activation of atypical protein kinase C ζ by caspase processing and degradation by the ubiquitin-proteasome system. *J. Biol. Chem.* **275**, 40620–40627 (2000).
23. Leitges, M. *et al.* Targeted disruption of the zetaPKC gene results in the impairment of the NF-κB pathway. *Mol. Cell* **8**, 771–780 (2001).
24. Su, I.H. & Tarakhovsky, A. Lysine methylation and 'signaling memory'. *Curr. Opin. Immunol.* **18**, 152–157 (2006).
25. Hirota, T., Lipp, J.J., Toh, B.H. & Peters, J.M. Histone H3 serine 10 phosphorylation by Aurora B causes HP1 dissociation from heterochromatin. *Nature* **438**, 1176–1180 (2005).
26. Fischle, W. *et al.* Regulation of HP1-chromatin binding by histone H3 methylation and phosphorylation. *Nature* **438**, 1116–1122 (2005).
27. Zhang, K. *et al.* The Set1 methyltransferase opposes Ipl1 aurora kinase functions in chromosome segregation. *Cell* **122**, 723–734 (2005).

ONLINE METHODS

Plasmids and reagents. For overexpression in mammalian cells, the plasmids were as follows: pCAG Flag-SETD6 wt, pCAG Flag-SETD6(Y285A), pCAG Flag-Smyd1, pCAG Flag-Smyd2, pCAG Flag-NSD2, pcDNA-RelA, pcDNA-RelA(K310R) and pcDNA Flag-GLP. The plasmid pcDNA3.1-GSV5-PKC-ζ(ca) was a gift from J. Smith. For *in vitro* assays, RelA(1–431) and RelA(430–551) were subcloned into pGEX-6P1. Single or double mutation of the sequence encoding RelA(1–431) was generated with the QuikChange site-directed mutagenesis kit (Stratagene), and sequences were confirmed by DNA sequencing. The pGEX-derived plasmids generated by mutagenesis were as follows: pGEX–RelA(K122R), pGEX-RelA(K123R), pGEX-RelA(K218R), pGEX-RelA(K221R), pGEX-RelA(K310R), pGEX-RelA(K314R,K315R) and pGEX-RelA(430–551). Sequence encoding p50 was subcloned into pGEX-6P1 by standard methods. All enzymes in the PKMT library are in **Supplementary Table 1**; enzymes used in **Figure 1a** and **Supplementary Figure 1** are in **Supplementary Table 2**. NSD1(SET) was a gift from D. Reinberg.

For expression in insect cells, cDNA encoding full-length SETD6 or various additional PKMTs was first cloned into pENTR3C and then recombined into Gateway pDEST20 with the Gateway LR Clonase II system (Invitrogen). Recombinant baculovirus were generated according to the manufacturer's protocol (Invitrogen). DH10Bac *Escherichia coli* cells were transfected with pDEST20 to generate recombinant baculovirus shuttle vector DNA. Sf9 *Spodoptera frugiperda* cells were then transfected with 2 μg baculovirus shuttle vector DNA with Cellfection II reagent (Invitrogen), and the baculovirus was amplified the times to obtain the optimal viral titer. For protein expression, baculovirus stocks were added to Sf9 cells grown in suspension at a density of 1×10^6 cells per ml, and transduced Sf9 cells were collected 2 d after transduction. Sf9 cells were maintained in Sf-900 II SFM media supplemented with 0.5% (vol/vol) penicillin-streptomycin.

Mouse RelA cDNA (Open Biosystems) was first cloned into the pENTR3C vector (Invitrogen) and then was recombined into the pBABE-FLAG-HA vector with the Gateway system as described above. RelA(K310R) was then generated with a QuikChange site-directed mutagenesis kit (Stratagene).

Cell lines, transfection and transduction of retrovirus or lentivirus. Human 293T and U2OS cells, mouse 3T3 cells (wild-type and *Rela*$^{-/-}$; a gift from M. Covert and T.D. Gilmore) and MEFs (wild-type and *Prkcz*$^{-/-}$; a gift from J. Moscat) were grown in DMEM (Gibco) supplemented with 10% (vol/vol) FCS (Gibco) and 100 units/ml of penicillin and L-glutamine. THP-1 cells (American Type Culture Collection) were cultured in RPMI-1640 medium (Gibco) supplemented with 10% (vol/vol) FCS (Gibco), 100 U/ml of penicillin and L-glutamine, 0.05 mM β-mercaptoethanol and 1× streptomycin. All cells were cultured at 37 °C in a humidified incubator with 5% CO_2. Cells were transfected with the TransIT transfection reagent (for plasmids; Mirus) or DharmaFECT reagent (for siRNA; Dharmacon), according to the manufacturer's protocols. Human SETD6–specific siRNA sequences were 5′-ACCTATGCCACAGACTTATT-3′ (1) and 5′-GACCACCACACTAAAGGTATT-3′ (2).

Mouse primary cells were isolated according to protocol 07064 of Rockefeller University and Institutional Animal Care and Use Committee protocol 9982 of Stanford University. Human biological samples were sourced ethically and their research use was in accordance with the terms of the informed consent received from each donor according to the Hertfordshire Ethics Committee Code 07/H0311/ 103. Mouse primary BMDMs were generated as described[28]. C57BL/6 bone marrow cells from femur and tibia were cultured for 7–8 d at 37 °C in 5% CO_2 in presence of 5 ng/ml of recombinant macrophage colony-stimulating factor and IL-3 (Peprotech). For knockdown experiments, siRNA directed against mouse SETD6 or control siRNA was transfected into cells with the HiPerFect transfection reagent according to the manufacturer's protocol (Qiagen), followed by stimulation experiments 48 h later. SETD6-specific siRNA sequences for BMDMs were 5′-GAACAAAGGATGAAACTGA-3′ (1) and 5′-GTGAGGAGGTGCTGACTGA-3′ (2). For human primary monocyte-derived dendritic cells, $CD14^+$ cells were separated with MACS CD14 beads (positive selection) according to the manufacturer's protocols (Miltenyi). After separation, $CD14^+$ cells were resuspended at a density of 1×10^6 cells per ml in RPMI-1640 medium (plus L-glutamine and 10% (vol/vol) heat-inactivated FCS) containing human recombinant granulocyte-monocyte colony-stimulating factor (30 ng/ml) and human recombinant IL-4 (20 ng/ml). Cells were differentiated for 5 d before transfection of siRNA by nucleofection according to the manufacturer's protocol (Amaxa) with the following minor alterations: siRNA was preplated into a 96-well U-bottomed plates with a final concentration of 2 μM. Monocyte-derived dendritic cells were resuspended in Amaxa Nucleofecter buffer at a density of 1×10^6 cells per 20 μl, and 20 μl of the suspension was added to the plate containing siRNA. The plate was placed into the Amaxa device and the monocyte program EA-100 was applied to all wells. After removal of the Amaxa plate, 100 μl prewarmed RPMI medium (plus 10% (vol/vol) heat-inactivated FCS, penicillin and L-glutamine) was added to each well, then cells were immediately removed from the Amaxa plate and added to a second flat-bottomed plate containing an additional 100 μl of prewarmed media. SETD6-specific siRNA sequences for monocyte-derived dendritic cells were 5′-TAATGCTGCCTCACGAACTGT-3′ (1) and 5′-TAGGAAATCCCAGCGCTCGTA-3′ (2). Mouse dendritic cells were isolated as described[29]. The FL-B16 mouse melanoma cells used to make the conditioned media were a gift from E. Engleman.

Cells were transduced with retrovirus and lentivirus as described[30]. Lentivirus for control, SETD6-specific and GLP-specific shRNA was from Santa Cruz Biotechnology. The human RelA shRNA target sequence is 5′-GATTGAGGAGAAACGTAAA-3′. For generation of the reconstituted cell lines, shRNA directed against the 3′ untranslated region of SETD6 was cloned into the shRNA vector pLentiLox3.7, and shRNA directed against wild-type SETD6 or SETD6(Y285A) was cloned into pWZL-3FLAG-hygro as an AscI-PacI cassette. U2OS and 3T3 cells were first transduced with pLentiLox SETD6 shRNA plasmid, followed by selection with puromycin (2 μg/ml). Puromycin-resistant cells were than transduced with pWZL-3Flag-SETD6 shRNA plasmid (wild-type SETD6 or SETD6(Y285A)) or with empty pWZL-hygro, followed by selection for 4 d with hygromycin B (250 μg/ml; Invitrogen). The SETD6 shRNA target sequences were 5′-CCTGTTCCCTGAAGGAACAGCAATA-3′ (human) and 5′-TGCTATTTGGCAGTTAGAATCAAAG-3′ (mouse). Where indicated, cells were stimulated with mouse TNF (10–20 ng/ml; R&D Systems) or LPS (10–100 ng/ml; Sigma).

Enzyme-linked immunosorbent and Luminex bead-based cytokine assays. Enzyme-linked immunosorbent assays were done as described[31] with anti-IL-6 (MP5-20F3; eBioscience) and anti-TNF (1F3F3D4; eBioscience). Plates were scanned with a SpectraMax 190 (Molecular Devices). Luminex standards were analyzed by multiplex bead-based arrays with the Mouse 26-Plex Multi-Cytokine Detection system (Panomics-Affymetrix) and with a Luminex 200 according to the manufacturer's protocol. Cytokine arrays were done at the Human Immune Monitoring Center of Stanford.

Gene-expression profiling. Gene expression arrays were done at the Stanford Functional Genomics Facility with a Mouse-Ref8 whole-genome array, according to the manufacturer's protocol (Illumina), and included two independent biological replicates (genes analyzed, **Supplementary Fig. 13**). Genes were selected when the mean change (fold) was over 1.5. *P* values for Venn and pie diagrams were calculated with Fisher's exact test and the χ^2 test, respectively.

***SETD6* mRNA in rheumatoid arthritis, septic shock and juvenile idiopathic arthritis.** A review of available literature involving microarray studies for rheumatoid arthritis, septic shock and juvenile idiopathic arthritis was used to identify four studies that met the criteria described below[32–37]. For rheumatoid arthritis, data were retrieved from the Stanford Microarray Database with the filtering criteria implemented before[32] and from the Gene Expression Omnibus database (accession code, GDS3628)[33]. Data were retrieved from the Gene Expression Omnibus database for septic shock (accession code, GSE8121)[35,37] and juvenile idiopathic arthritis (accession codes, GSE13501 and GSE13849)[34]. Only studies with microarray platforms that contained *SETD6* probes were considered[36]. In the study selected for its data on rheumatoid arthritis[32], which used custom cDNA microarrays deposited in Stanford Microarray Database, initial analysis showed that two of the three *SETD6* probes on the array (IMAGE 213233 and IMAGE 66711) were of poor quality because of a low signal/background ratio in both channels (mean ratio, 3.7 and 5.1, respectively; this resulted in the removal of many data points by the filtering threshold of 2.5 used[32]), and these results were therefore removed from the analysis.

The remaining probe (IMAGE 1699773) had a much higher mean ratio (13.5), well above the threshold, and was thus used in the analysis. Final normalized data were retrieved from either of the databases noted above with filtering criteria described in the respective publications[36]. The results of any data sets containing multiple high-quality probes representing *SETD6* were averaged before statistical analysis. For analysis of significance, a two-tailed independent *t*-test with unequal variance was applied to each study containing a comparison between a disease group and a healthy control group or, in one case, patients with rheumatoid arthritis that responded to infliximab versus patients whose rheumatoid arthritis did not respond to infliximab.

***In vitro* lysine-methylation assay.** These assays were done as described[38]. Recombinant RelA derivatives and peptides, recombinant nucleosomes (a gift from R. Kingston and M. Simon) or purified nucleosomes of HeLa cervical cancer cells[39] were incubated overnight at 30 °C with recombinant PMKTs and 0.1 mM S-adenosyl-methionine (AdoMet; Sigma) or 2 mCi ^{3}H-labeled S-adenosyl-methionine (AdoMet; Amersham) in methylation buffer containing 50 mM Tris-HCl, pH 8.0, 10% (vol/vol) glycerol, 20 mM KCl, 5 mM MgCl2 and 1 mM phenylmethyl sulfonyl fluoride. Reaction mixtures were resolved by SDS-PAGE, followed by autoradiography, immunoblot analysis or Coomassie staining (Pierce). Reactions with peptides were analyzed by dot blot or mass spectrometry.

Mass spectrometry. Before mass spectrometry, peptides were diluted in 0.1% (vol/vol) acetic acid for desalting with C18 stage tips ('stop and go' extraction tips) made in-house as described[40]. Samples were then loaded with an Eksigent AS2 autosampler into fused silica capillary columns (inner diameter, 75 μm) packed with 15 cm of C18 reversed-phase resin (5 μm in diameter with a pore size of 200 Å; Magic C18; Michrom BioResources). Capillary columns were constructed with an electrospray tip for nanoflow reversed-phase high-performance liquid chromatography–tandem mass spectrometry on a hybrid linear quadrupole ion-trap Orbitrap mass spectrometer (Thermo Electron). Peptides were resolved with a gradient of 5–35% buffer B in 110 min gradient (buffer A, 0.1 M acetic acid; buffer B, 70% (vol/vol) acetonitrile in 0.1 M acetic acid) with a flow rate of approximately 200 nl/min on an Agilent 1200 binary HPLC system.

The Orbitrap was operated with a resolution of 30,000 for a full mass spectrometry spectrum, followed by seven subsequent data-dependent tandem mass spectrometry spectra collected in the ion trap after electron transfer dissociation of peptides. Peptides selected for tandem mass spectrometry were put on an exclusion list for 60 s to avoid duplicate spectra. All spectra were analyzed with Qual Browser (version 2.0.7, Thermo Scientific), and the identity of each peptides was confirmed by manual inspection of tandem mass spectrometry spectra.

Interaction studies, immunoblot analysis, calf intestinal alkaline phosphatase assays, kinase assays and antibodies. Cell extracts were prepared by lysis of PBS-washed cells in radioimmunoprecipitation assay lysis buffer (50 mM Tris-HCl, pH 8, 150 mM NaCl, 1% (vol/vol) Nonidet P-40, 0.5% (vol/vol) deoxycholate, 0.1% (vol/vol) SDS, 1 mM dithiothreitol and protease inhibitor 'cocktail' (diluted 1:100; P8340; Sigma). Protein concentrations were measured with the Bradford reagent (Bio-Rad). Equal amounts of protein for each sample were mixed with Laemmli sample buffer (4% (vol/vol) SDS, 20% (vol/vol) glycerol, 10% (vol/vol) 2-mercaptoethanol and 0.125 M Tris·HCl, pH 6.8), then were heated for 5 min at 95 °C and separated by SDS-PAGE.

For analysis of the presence of monomethylated Lys310 and phosphorylated Ser311 on the same molecule, immunoprecipitated endogenous RelA from 293T cells transfected with PKC-ζ(ca) was washed three times with radioimmunoprecipitation assay buffer. Immunoprecipitated RelA bound on protein A–protein G beads was separated into two equal aliquots that were mock treated or were treated for 1 h at 37 °C with calf intestinal alkaline phosphatase (New England Biolabs) before immunoblot analysis. Recombinant PKC-ζ for the kinase assays was from Invitrogen (P2268). Biochemical fractionation, glutathione *S*-transferase precipitation assays, immunofluorescence staining, and protein-protein ChIP experiments were done as described[38,41,42].

Antibodies used were as follows: anti-GLP (sc-81260; Santa Cruz Biotechnology), anti-p65 (sc-8008 AC; Santa Cruz Biotechnology), anti-Flag (F3165; Sigma-Aldrich), anti-GLP (09-078; Millipore), anti-GLP (A301-642A-1; Bethyl), horseradish peroxidase–linked anti–glutathione *S*-transferase (ab3416; Abcam), anti-H3 (ab1791; Abcam); horseradish peroxidase–linked anti-V5 (ab1325; Abcam), anti-p65 (ab16502; Abcam), antibody to p65 phosphorylated at Ser311 (ab51059, Abcam), anti-H3K9me2 (ab1220; Abcam), anti-PKC-ζ (ab4137, Abcam), antibody to p65 phosphorylated at Ser311 (ab-311; GenScript), anti-β-tubulin (05-661; Millipore), and anti-β-actin (A1978; Sigma-Aldrich). Rabbit polyclonal antibody to RelAK310me1 was elicited by the peptide sequence TYETFK$_{me1}$SIMKKSPC (where subscripted 'me1' indicates Lys310; Century Biochemical). Rabbit polyclonal antibody to SETD6 was elicited by glutathione *S*-transferase–linked SETD6 (Covance).

ChIP. A published protocol was used for ChIP[43]. Formaldehyde-crosslinked protein-DNA complexes were precipitated by incubation overnight with the appopriate antibody or with rabbit immunoglobulin G (negative control); 15506; Sigma-Aldrich. Precipitated DNA fragments were isolated with Chelex 100 resin (BioRad) as described[44] and were amplified by quantitative real-time PCR (ABI PRISM 7700 Sequence Detection System; primers, **Supplementary Table 3**).

Luciferase assay. Cells were transiently transfected with the appropriate combinations of plasmids. The total amount of transfected DNA in each dish was kept constant by the addition of empty vector where necessary. Cell extracts were prepared 24 h after transfection, and luciferase activity was measured with the Dual-Glo Luciferase Assay system (Promega) and normalized to that of renilla luciferas. The κB-luc luciferase reporter plasmid was provided by W.C. Greene.

RNA extraction and reverse transcription. RNA was prepared with an RNeasy Plus kit (Qiagen) and was reverse-transcribed with the SuperScript III First-Strand Synthesis system (Invitrogen). Quantitative real-time RT-PCR was done in triplicate on an ABI PRISM 7700 Sequence Detection system with TaqMan Gene Expression Assay primer and probe sets (Applied Biosystems). Results were normalized to the abundance of *Gapdh* (encoding glyceraldehyde phosphate dehydrogenase).

Isothermal titration calorimetry. GLP(ANK) was concentrated to 24 μM in 150 mM NaCl and 20 mM Tris, pH 8.0, followed by isothermal titration calorimetry at 25 °C with 370–475 μM peptide on a MicroCal VP-ITC instrument. Binding constants were calculated by fitting of the data with the ITC Data Analysis module of Origin 7.0 scientific plotting software (OriginLab).

Homology modeling of SETD6. PHYRE server 23 (protein homology-analogy recognition engine)[45] was used for homology modeling for SETD6. Among the models with the highest confidence scores (e-value, 1.73×10^{-28}), a homology model of SETD6 readily gave a solution with the structure of plant enzyme LMST (Rubisco large subunit methyltransferase) bound to S-adenosyl-methionine and lysine (Protein Data Bank accession number, 2H2E)[46].

Peptide precipitation and peptide or protein array. Biotinylated histone peptides, peptide microarray experiments and peptide-precipitation assays were done as described[47]. CADOR protein microarrays were generated as described[48]. RelA peptides were synthesized at the Yale W.M. Keck facility. The sequence of RelA(300–320) was biotin-EKRKRTYETFK#S*IMKKSPFSG; Lys310 (K#) was unmodified, monomethylated, dimethylated or trimethylated, and Ser311 (S*) was unmodified or phosphorylated.

Growth curves and soft-agar assay. For growth curves, 5×10^4 to 20×10^4 cells were plated in triplicate and cells were counted every day for 5–7 d with a hemocytometer. For soft-agar assays, 2×10^4 cells were plated in triplicate in 0.8% (wt/vol) agarose on a base agar medium of 3% (wt/vol) agarose. Colony formation was quantified after 21 d as the numbers of colonies per field.

28. Toney, L.M. *et al.* BCL-6 regulates chemokine gene transcription in macrophages. *Nat. Immunol.* **1**, 214–220 (2000).
29. Yasuda, K. *et al.* Murine dendritic cell type I IFN production induced by human IgG-RNA immune complexes is IFN regulatory factor (IRF)5 and IRF7 dependent and is required for IL-6 production. *J. Immunol.* **178**, 6876–6885 (2007).
30. Michishita, E. *et al.* SIRT6 is a histone H3 lysine 9 deacetylase that modulates telomeric chromatin. *Nature* **452**, 492–496 (2008).

doi:10.1038/ni.1968

31. Kattah, M.G., Coller, J., Cheung, R.K., Oshidary, N. & Utz, P.J. HIT: a versatile proteomics platform for multianalyte phenotyping of cytokines, intracellular proteins and surface molecules. *Nat. Med.* **14**, 1284–1289 (2008).
32. van der Pouw Kraan, T.C. *et al.* Rheumatoid arthritis subtypes identified by genomic profiling of peripheral blood cells: assignment of a type I interferon signature in a subpopulation of patients. *Ann. Rheum. Dis.* **66**, 1008–1014 (2007).
33. Julia, A. *et al.* An eight-gene blood expression profile predicts the response to infliximab in rheumatoid arthritis. *PLoS One* **4**, e7556 (2009).
34. Barnes, M.G. *et al.* Subtype-specific peripheral blood gene expression profiles in recent-onset juvenile idiopathic arthritis. *Arthritis Rheum.* **60**, 2102–2112 (2009).
35. Wong, H.R. *et al.* Genome-level expression profiles in pediatric septic shock indicate a role for altered zinc homeostasis in poor outcome. *Physiol. Genomics* **30**, 146–155 (2007).
36. Demeter, J. *et al.* The Stanford Microarray Database: implementation of new analysis tools and open source release of software. *Nucleic Acids Res.* **35**, D766–D770 (2007).
37. Shanley, T.P. *et al.* Genome-level longitudinal expression of signaling pathways and gene networks in pediatric septic shock. *Mol. Med.* **13**, 495–508 (2007).
38. Shi, X. *et al.* ING2 PHD domain links histone H3 lysine 4 methylation to active gene repression. *Nature* **442**, 96–99 (2006).
39. Schnitzler, G.R. in *Current Protocols in Molecular Biology* Ch 21, 21.5.1–21.5.12 (John Wiley & Sons, Hoboken, New Jersey, 2001).
40. Rappsilber, J., Ishihama, Y. & Mann, M. Stop and go extraction tips for matrix-assisted laser desorption/ionization, nanoelectrospray, and LC/MS sample pretreatment in proteomics. *Anal. Chem.* **75**, 663–670 (2003).
41. Mendez, J. & Stillman, B. Chromatin association of human origin recognition complex, cdc6, and minichromosome maintenance proteins during the cell cycle: assembly of prereplication complexes in late mitosis. *Mol. Cell. Biol.* **20**, 8602–8612 (2000).
42. Michishita, E., Park, J.Y., Burneskis, J.M., Barrett, J.C. & Horikawa, I. Evolutionarily conserved and nonconserved cellular localizations and functions of human SIRT proteins. *Mol. Biol. Cell* **16**, 4623–4635 (2005).
43. Ainbinder, E. *et al.* Mechanism of rapid transcriptional induction of tumor necrosis factor α-responsive genes by NF-κB. *Mol. Cell. Biol.* **22**, 6354–6362 (2002).
44. Nelson, J.D., Denisenko, O. & Bomsztyk, K. Protocol for the fast chromatin immunoprecipitation (ChIP) method. *Nat. Protocols* **1**, 179–185 (2006).
45. Kelley, L.A. & Sternberg, M.J. Protein structure prediction on the web: a case study using the Phyre server. *Nat. Protocols* **4**, 363–371 (2009).
46. Couture, J.F., Hauk, G., Thompson, M.J., Blackburn, G.M. & Trievel, R.C. Catalytic roles for carbon-oxygen hydrogen bonding in SET domain lysine methyltransferases. *J. Biol. Chem.* **281**, 19280–19287 (2006).
47. Bua, D.J. *et al.* Epigenome microarray platform for proteome-wide dissection of chromatin-signaling networks. *PLoS One* **4**, e6789 (2009).
48. Espejo, A., Cote, J., Bednarek, A., Richard, S. & Bedford, M.T. A protein-domain microarray identifies novel protein-protein interactions. *Biochem. J.* **367**, 697–702 (2002).